Phonon instabilities in rocksalt AgCl and AgBr under pressure studied within density functional theory

Yan Li, Lijun Zhang, Tian Cui, Yanming Ma,* and Guangtian Zou
National Laboratory of Superhard Materials, Jilin University, ChangChun 130012, People's Republic of China

Dennis D. Klug
Steacie Institute for Molecular Sciences, National Research Council of Canada, Ottawa, Ontario, Canada K1A 0R6

(Received 10 May 2006; revised manuscript received 6 July 2006; published 4 August 2006)

The phonons and elastic constants of rocksalt AgCl and AgBr under pressure are extensively studied by using the pseudopotential plane-wave method within density functional theory. A pressure-induced soft transverse acoustic (TA) phonon mode is identified for both compounds. Interestingly, each compound shows a different phonon softening behavior. A TA phonon branch softens to zero pressure at 6.5 GPa along [ξ00] direction in AgCl, resulting in the phase transition from the rocksalt structure to the monoclinic structure. A softening TA phonon mode at the zone boundary *X* point in AgBr is predicted and the deduced transition pressure of ~9.8 GPa is found to be 24% larger than the experimental measurement of ~7.9 GPa. The predicted larger transition pressure indicated that the TA softening phonon mode at the zone boundary *X* point in AgBr may not independently induce the phase transition. Moreover, a pressure-induced softening of shear modulus in C_{44} is also verified for both compounds. However, it is suggested that the phonon instability, instead of C_{44} instability, dominates the pressure-induced structural phase transition.

DOI: 10.1103/PhysRevB.74.054102 PACS number(s): 62.50.+p, 63.20.Dj, 64.70.Kb

The structural behavior of binary *AB* compounds under hydrostatic pressure has been a popular topic in condensed matter research over the past decade. The most covalent *AB* compounds are the III-V and II-VI semiconductors which, at ambient conditions, generally adopt the tetrahedrally coordinated zinc blende (ZB) or wurtzite structure. By analogy with the behavior of elemental Si and Ge under compression, many of these phases were originally thought to adopt a diatomic version of the tetragonal β-Sn structure at high pressure.[1,2] However, the recent advent of angle-dispersive x-ray diffraction techniques through the diamond anvil cells[3,4] has surprisingly revealed that the previous assignments of the β-Sn structure to compound semiconductors are incorrect.[5] At the other extreme, the highly ionic Na, K, and Rb halides adopt the rocksalt structure at ambient conditions and, under pressure, the majority of these compounds undergo first-order structural phase transitions from sixfold to the eightfold coordinated CsCl structure.[6]

In contrast to the general picture given above, the high-pressure structural behavior of compounds whose bonding character is intermediate between ionic and covalent is often rather complex.[7] This is the case for the silver halides, which can be considered as I-VII compounds lying at the ionic end of the sequence IV $\rightarrow$ III-V $\rightarrow$ I-VII. Silver halides are of great physical interest in normal and high pressure investigations, since they act as photographic materials, solid electrolytes, and as liquid semiconductors.[8] Under ambient conditions, AgF, AgCl, and AgBr crystallize in the rocksalt structure characteristic of ionic bonding, while AgI exists as two-phase mixture of the cubic ZB polymorph and its hexagonal wurtzite counterpart. The Ag atom possesses a completely filled $4d^{10}$ shell and a single 5*s* electron which is transferred to the halide atom. Thus, the structural behaviors of AgCl and AgBr under pressure are different from that of alkali halides because the 4*d* electrons of the Ag atom hybridize with the halide *p* state.

There are many theoretical and experimental investigations related to phase transition of AgCl and AgBr under pressure.[7–14] In the very earlier experiments before 1960, both compounds have been found to undergo a first-order transformation around 8–9 GPa and it was suggested to be a transformation to the CsCl structure.[9,10] This is the behavior known for alkali halides which are ionic. In 1969, Schock *et al.*'s experiments[11] suggested that this first-order transformation might go to a hexagonal phase with a cinnabar structure.[12] However, very recently, using angle-dispersive x-ray diffraction measurements, Hull *et al.*[7] accurately demonstrated that the rocksalt-structured AgCl and AgBr undergo the first phase transition to a monoclinic structure with KOH-type arrangement at 6.6 GPa and 7.9 GPa, respectively. On the theoretical side, Gupta *et al.*[13] employed a three-body-potential approach to describe the phase transitions and equation of states (EOS) for AgCl and AgBr. However, they suggested that the rocksalt structure will transform directly to the CsCl structure based on the structural similarities between the alkali halides and the silver halides. While Nunes *et al.*[14] later suggested that AgCl and AgBr might prefer a rhombohedral phase induced from the rocksalt structure with pressure. Up to now, to the best of our knowledge, the physically driven mechanism of the pressure-induced structural phase transition from the rocksalt structure to the monoclinic structure for AgCl and AgBr remains unclear. Dynamic instabilities are often responsible for phase transitions under pressure.[15,16] Lattice dynamics therefore plays an important role in understanding the mechanisms of phase transitions. In our previous works,[17,18] the different mechanisms driving the phase transitions in copper halides from ZB CuCl-II to cubic CuCl-IV, from ZB CuBr-III to a tetragonal phase CuBr-IV, and from ZB CuI-III to a rhombohedral phase CuI-IV are clearly revealed by the accurate *ab initio* determination of the transverse acoustic (TA) phonon soften-

TABLE I. Calculated equilibrium lattice parameter (a_0), bulk modulus (B_0), and the pressure derivative of bulk modulus ($\mathbf{B}'_0$) for AgCl and AgBr, respectively. Previous theoretical calculations from Ref. 14 and experimental results from Ref. 26–30 are also shown for comparison. The units for a_0 and B_0 are in Å and Mbars, respectively.

		a_0 (Å)	B_0 (Mbar)	B'_0
AgCl				
	This work	5.67	0.41	4.97
	Ref. 14	5.41	0.67	5.98
	Exp.	5.55[a]	0.51[b]	5.20[c]
AgBr				
	This work	5.90	0.38	4.90
	Ref. 14	5.64	0.60	5.10
	Exp.	5.75[a]	0.41[d]	8.50[e]

[a]Reference 26.
[b]Reference 27.
[c]Reference 28.
[d]Reference 29.
[e]Reference 30.

ing at the zone boundary X and L for CuCl and CuI, respectively, and along the $[\xi\xi 0]$ direction for CuBr in the first Brillouin zone (BZ). Consequently, in this work, *ab initio* investigations of lattice dynamics are, thus, carried out to probe the nature of pressure-induced phase transformation in rocksalt AgCl and AgBr.

The lattice dynamics for both compounds are investigated using the pseudopotential plane-wave density-functional linear-response method.[19] The generalized gradient approximation (GGA) of the exchange-correlation functional is used.[20] The Troullier-Martins[21] norm-conserving scheme is used to generate the tight pseudopotentials for Ag, Cl, and Br with electronic configurations of $4d^{10}5s^1$, $3s^23p^5$, and $4s^24p^5$, respectively. Smaller core radii are chosen as 2.42 a.u. for s and d orbtials for Ag, 1.59 a.u. for s and p orbitals for Cl, 1.77 and 2.09 a.u. for s and p orbitals for Br, respectively, to guarantee the nonexistence of core overlapping under highest pressure in this study. The convergence tests gave the kinetic energy cutoffs of 110 Ry and 120 Ry for AgCl and AgBr, respectively, with a $8\times8\times8$ Monkhorst-Pack (MP) grid for the electronic BZ integration. A $4\times4\times4$ q mesh in the first BZ is used in the interpolation of the phonon calculations. The elastic constant tensors were calculated as a function of pressure using the stress-strain relations for AgCl and AgBr as implemented in the Materials Toolkit2.1.[22,23] Elastic constants were obtained from evaluations of the stress tensor generated by small strains using the density-functional plane wave technique as implemented in the VASP code.[24] The GGA projector augmented wave (PAW) potentials[25] were used with $8\times8\times8$ or $12\times12\times12$ Monkhorst-Pack k-point meshes.

The theoretical equilibrium lattice constants and EOS in rocksalt AgCl and AgBr are determined by fitting the total energies as a function of volume to the Murnahan EOS. The calculated equilibrium lattice parameters and bulk modulus, together with another pseudopotential plane-wave theoretical calculation within local density approximation (LDA) and the experimental data are listed in Table I. It is found that the current theoretical lattice constant and bulk modulus are in good agreement with experimental data within 3%, thus, it strongly supports the choice of pseudopotentials and the GGA approximation for the current study. It is worth noting that the current theoretical lattice constants are larger than those of experimental results, while it is smaller in Ref. 14. They are the typical deviation of GGA and LDA calculations, respectively. The calculated EOS of AgCl and AgBr in rocksalt structure are compared with the experimental data[7] as shown in Fig. 1. The agreement between theoretical results and the experimental data is also satisfactory, lending another strong support in the validity of the current theoretical model.

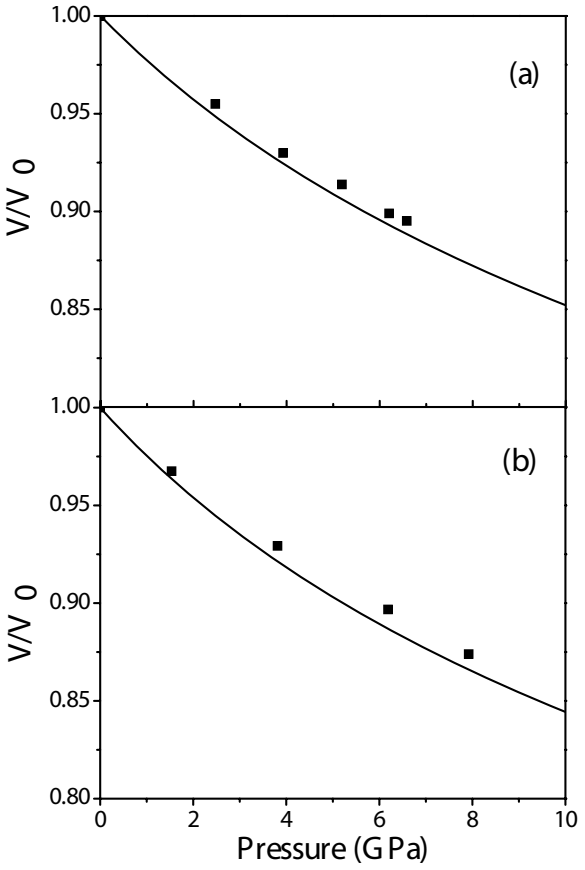

FIG. 1. Comparison of the calculated equation of states (solid line) for AgCl (a) and AgBr (b) with the experimental data (solid square symbols) from Ref. 7.

Figure 2 shows the comparison of our *ab initio* phonon dispersion curves and one-phonon density of states (DOS) for AgCl at the experimental lattice constant of 5.55 Å with the experimental neutron inelastic scattering data at zero pressure.[31] It is clear that the present *ab initio* calculations accurately predict the phonon frequencies at zero pressure. In particular, the shoulder in the longitudinal optical (LO) ($[\xi\xi 0]$) branch near the K point, the low-lying transverse optical (TO) branch along the direction of $[\xi\xi\xi]$, and the minimum in the LO branch along the direction of $[\xi 00]$ are correctly reproduced in theory. With the addition of the

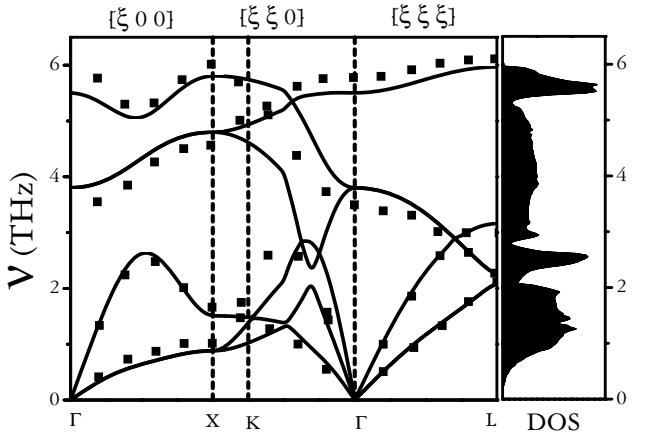

FIG. 2. The calculated phonon frequencies (solid lines) and vibrational DOS of AgCl at ambient pressure, along with the experimental phonon dispersion data (symbols) at $T=78$ K (Ref. 31).

nonanalytic term to the dynamical matrix, the longitudinal optic branch and the transverse optic branch split from each other at the Γ point, and this is also shown. The calculated phonon dispersions at the experimental lattice constant of 5.75 Å and one-phonon density of DOS for AgBr, along with the experimental phonon data[32] are presented in Fig. 3. The calculated phonon disperson agrees well with experiments, except for the somewhat larger discrepancy in the TO phonon branch. For the L point, it has been previously found that the TO and TA branches exchange their eigenvectors.[33] In this case, the heavier Ag^+ ion oscillates with the higher frequency while the lighter Br^- oscillates with the lower frequency, with a ratio of 0.80 in the Br^- to the Ag^+ frequency. This behavior clearly shows that there are different forces involved in these two modes. A determination of the relative intensities of TA to TO at L point by inelastic neutron scattering directly proved the exchange of eigenvectors, as was concluded from exciton recombination luminescence and resonant Raman scattering from excitons in AgBr[34] which couple to phonons. Note that the present calculations correctly reveal this change of eigenvectors.

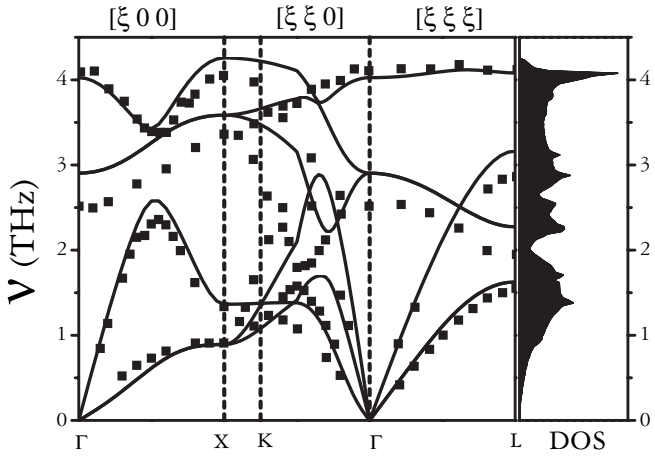

FIG. 3. The calculated phonon frequencies (solid lines) and vibrational DOS of AgBr at ambient pressure, together with the experimental phonon dispersion data (symbols) at $T=85$ K (Ref. 32).

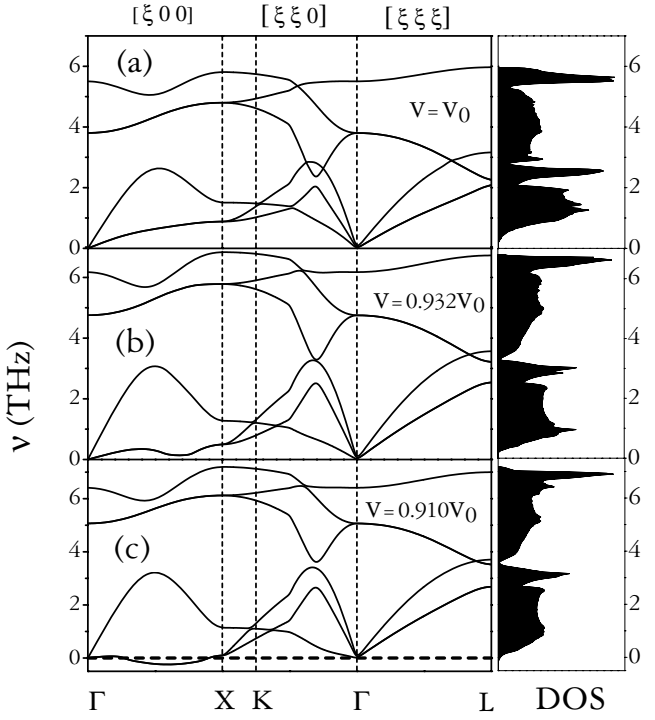

FIG. 4. Calculated phonon frequencies and vibrational DOS of AgCl at different volumes.

The calculated phonon dispersion curves of AgCl and the one-phonon DOS at different volumes are shown in Fig. 4. One observes that with decreasing volume, the TO, LO, and longitudinal acoustic (LA) phonon modes shift to higher frequencies, while the TA phonon branch along the [ξ00] direction decreases in frequency, indicating a negative mode Grüneisen parameter, $\gamma_j(q)=-\partial \ln \upsilon_j(q)/\partial \ln V$ for mode j, where q is wave vector, ν is frequency, and V is volume. At a volume of $0.910V_0$ (V_0, experimental equilibrium volume), the phonon frequencies of the TA modes along the [ξ00] direction decrease to be imaginary, signaling a structural instability in the rocksalt phase. Figure 5 shows the variation of the frequency of the TA (q) mode for the most negative q(0.6 0.0 0.0) point in Fig. 4(c) with pressure. The estimated transition pressure is ~6.5 GPa ($V=0.915V_0$) from Fig. 5 which is in excellent agreement with the experimental transition pressure of ~6.6 GPa,[7] thus signifying the phase transition from the rocksalt structure to the monoclinic structure. The squared phonon frequencies ν^2 for the TA branch at the q(0.6 0.0 0.0) point with pressure P are also plotted as shown in the inset (a) of Fig. 5. A near perfect linear relation between ν^2 and P is obtained. Such behavior is consistent with the Landau theory of pressure-induced soft mode phase transitions.[33] The schematic representation of eigenvectors for the TA phonon mode at the q(0.6 0.0 0.0) point is shown in the inset (b) of Fig. 5. The arrows represent the directions of the atomic vibrations for the Ag cation and its six nearest neighboring Cl anions, respectively. Inspection of the phonon eigenvectors shows that this mode involves alternate shuffles of (100) planes in the direction along the direction of [001]. Phonon softening usually corresponds to the instability of a particular atomic movement. The rocksalt structure

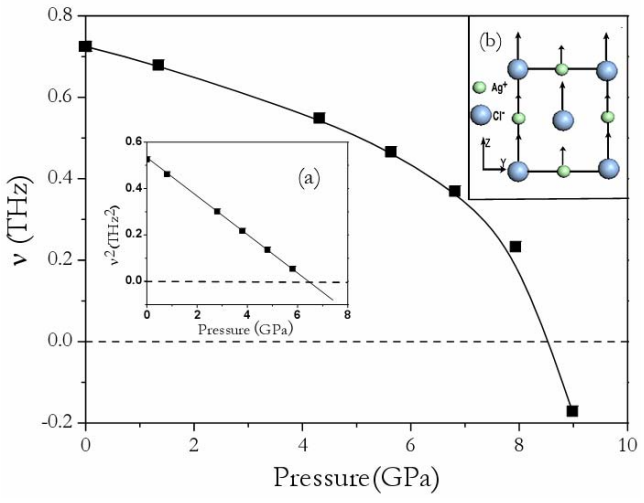

FIG. 5. (Color online) Main figure: Calculated TA phonon frequencies at the q (0.6 0.0 0.0) point of BZ in AgCl as a function of volume. Solid line through the calculated data points represents fitted curves using a B spline. Inset: (a) the calculated squared phonon frequency ν^2 as a function of pressure. Solid line through the data points is a linear fit; (b) the eigenvector for TA soft phonon mode at the q (0.6 0.0 0.0) point. The displacements are all in the (100) plane. The Ag cations and the Cl anions all move along the [001] direction. The arrows show the directions of atomic displacements.

AgCl, therefore, tends to become unstable with respect to the atomic displacement corresponding to the soft mode. The atomic movements along the directions of the eigenvectors in the (100) planes is closely related to the phase transition from the rocksalt structure to the monoclinic structure. Ozoliņš *et al.*[15] found a soft TA mode at the X(1.0 0.0 0.0) point for rocksalt GaP under pressure using the first-principles LDA linear response approach. Their predicted soft mode also involves shuffles of (100) planes along the [001] direction, similar to our current findings in AgCl. They proposed that the phonon softenings are dominated by the competition between the attractive electrostatic Madelung energy and the repulsive short-range energy acting between the nearest neighbors. The shear-type corresponding to the softening mode TA(X), can lower the repulsive energy [contributing to $\gamma_{TA}(X)<0$] and raises the Madelung energy [contributing to $\gamma_{TA}(X)>0$].[15] Since the repulsive energy changes much faster than the Madelung energy upon decreasing **R**, it leads to $\gamma_{TA}(X)<0$, which for sufficient compression, causes an instability $\nu_{TA}^2(X)<0$.[15] Due to the similarity in the atomic vibrations corresponding to the soft modes in these two calculations, the predicted soft mode with wave vector of (0.6 0.0 0.0) in AgCl might be also attributed to the same competition mechanism adopted by GaP.

Figure 6 shows the calculated phonon dispersion curves and one-phonon DOS for AgBr at several volumes. It is interestingly noted that with increasing pressure the TA phonon frequency at the zone boundary X (0.0 0.0 1.0) point decreases, while other phonon modes shift to higher energy. At $V=0.881V_0$ (V_0, experimental equilibrium volume), the TA phonons at the X point soften to imaginary frequencies, indicating a structural instability. Figure 7 shows the variation of the frequency of the TA(X) mode with volume. The squared phonon frequencies ν^2 for the TA branch at the X

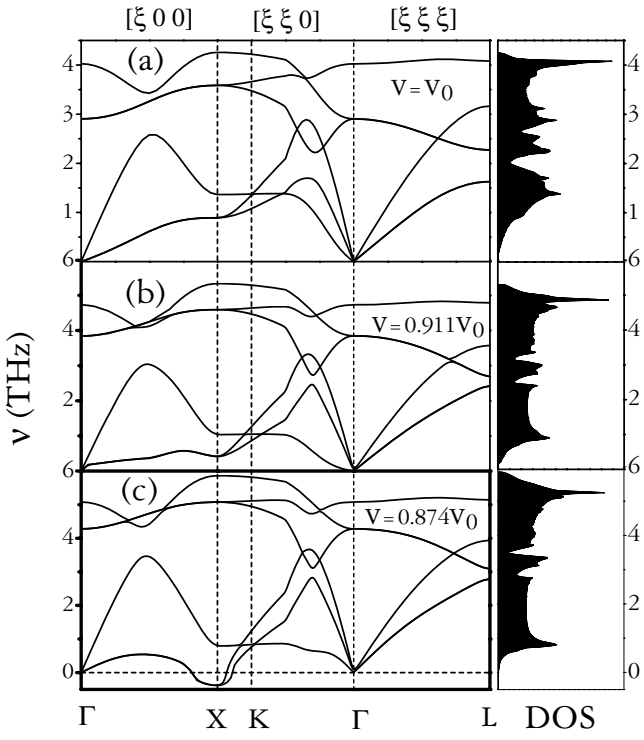

FIG. 6. Calculated phonon dispersion curves and vibrational DOS of AgBr at different volumes.

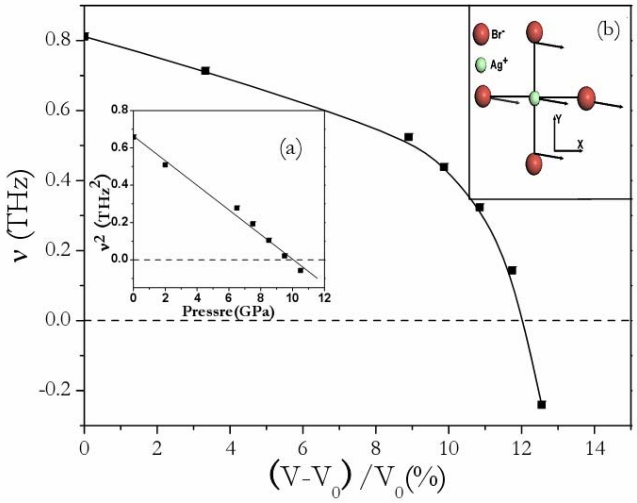

FIG. 7. (Color online) Main figure: Calculated TA phonon frequencies at the X (1.0 0.0 0.0) point of BZ in AgBr as a function of volume. Solid line through the calculated data points represents fitted curves using a B spline. Inset: (a) the calculated squared phonon frequency ν^2 as a function of pressure. Solid line through the data points is a linear fit. (b) the eigenvector for TA soft phonon mode at the X (1.0 0.0 0.0) point. The Ag atom is located at (0 0 0). The other four Br atoms sit at (1/2 0 0), (−1/2 0 0), (0 1/2 0), and (0 −1/2 0), respectively. The eigenvectors of the Ag cation and Br anion are antiparallel in the primitive cell and the eigenvector of the Ag cation forms an angle 14.1° with respect to the [001] direction.

TABLE II. Calculated elastic constants of C_{11}, C_{12}, C_s, and C_{44} with GPa unit for AgCl and AgBr at ambient pressure. For AgCl, the available experimental data are taken from Ref. 35. For AgBr, experimental data are taken from Ref. 37.

		C_{11}	C_{12}	C_{44}	C_s
AgCl	Expt.	59.6	36.2	6.21	11.7
	This work	61.4	44.8	6.14	8.18
	Expt.	63.1	34.1	7.65	14.5
AgBr	This work	73.8	42.4	7.71	15.7
	Ref. 37	64.1	35.2	8.40	14.5

point with pressure P are also plotted as shown in the inset (a) of Fig. 7. A near perfect linear relation between ν^2 and P is also obtained. The estimated transition pressure is ~9.8 GPa ($V=0.874V_0$), which is 24% larger than the experimental transition pressure of ~7.9 GPa. This somewhat large difference indicates that the phase transition from the rocksalt structure to the monoclinic structure may not be induced independently by the phonon instability at the zone boundary X point. This behavior of the phonon softening to zero frequency is hidden by the first order phase transition to the monoclinic phase. Although this phase transition occurs at pressures below those required to drive the TA modes to zero frequency, the "mode-softening" behavior may be related to the particular mechanism. The schematic representation of eigenvectors for the TA soft phonon mode at the X point is shown in the top view of the (001) plane of rocksalt structure in the inset (b) of Fig. 7. The eigenvectors of the Ag cation and Br anion are antiparallel in the primitive cell and the displacement of the Ag cation forms an angle 14.1° with respect to the direction [100]. We remark that one possible physically driving mechanism for AgBr from the rocksalt structure to the monoclinic structure may be partly related to a shear instability with atomic displacements forming angle 14.1° with respect to the [100] direction.

Table II lists the calculated elastic constants for rocksalt AgCl and AgBr with the experimental data[35,36] and previously theoretical results[37] in AgBr at ambient pressure. It is clear that there is an excellent agreement in C_{44} for both compounds and in $C_s=1/2(C_{11}-C_{12})$ for AgBr between the calculated results and the experimental measurements. However, there are noticeably larger discrepancies in C_{11} and C_{12} for AgBr and in C_s for AgCl. The larger discrepancy might be mainly attributed to the differences in the equilibrium lattice constants between theory and experiment. Nevertheless, the accurate determination of the C_{44} by theory at ambient pressure for both compounds lends a strong support for examination of its high pressure behavior. The variations of the elastic constants with pressure for rocksalt AgCl and AgBr are shown in Figs. 8 and 9, respectively. One observes that C_{11}, C_{12}, and C_s show linearly increasing trends with pressure for both compounds, while C_{44} shows a linear softening trend. It is interesting to note that the extrapolation of C_s to small negative pressures of −2.0 and −2.9 GPa, corresponding to larger lattice constants of 5.669 and 5.965 Å for AgCl and AgBr, respectively, will induce C_s instabilities for both compounds. The theoretical elastic constants with pressure for AgBr from Ref. 37 are also plotted in Fig. 9 for comparison. It is found that the calculated elastic constants with pressure are in quantitive agreement with those from Ref. 37 except for the apparent deviation from the linear trend around 2.8 GPa for C_{11} and C_{12} in their calculations. Specifically, at higher pressure, the two theoretical calculations for C_{12} and C_{44} agree well each other, while the current results for C_{11} and C_s are smaller. It is worth noting that although C_{44} softens with pressure for both compounds, it still remains positive under pressures at which the phonons soften to zero frequency for AgCl (6.5 GPa) and AgBr (9.8 GPa). It should be also pointed out that for both compounds, the phonon instabilities occur at points away from the center of the Brillouin zone and appear before the materials become unstable according to elastic stability criteria. Therefore, it is concluded that the pressure-induced structural

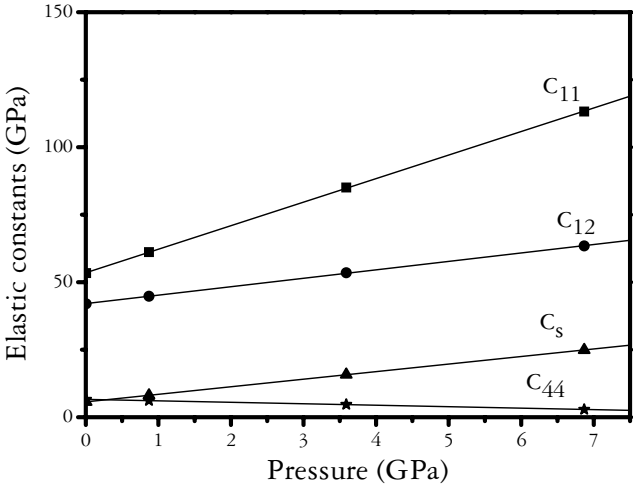

FIG. 8. Calculated elastic constants (solid symbols) of C_{11}, C_{12}, C_s, and C_{44} for AgCl with pressure in rocksalt structure. The solid lines are the linear fits to the calculated results.

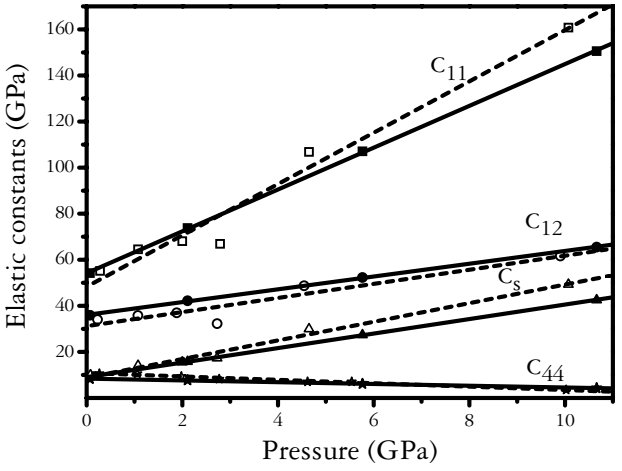

FIG. 9. Calculated elastic constants (solid symbols) of C_{11}, C_{12}, C_s, and C_{44} for AgBr with pressure in rocksalt structure. The solid lines are the linear fits to the calculated results. The open symbols are taken from a previous calculation in AgBr from Ref. 37. The dashed lines are the linear fits to their theoretical results.

phase transition for both compounds is not induced by the C_{44} instabilities which are related to the long-wavelength part of the transverse branch near the center of the first BZ.

In conclusion, the phonon dispersion curves for AgCl and AgBr are calculated at different volumes using density functional linear-response theory. For AgCl, TA phonon instabilities along the $[\xi 00]$ direction of the first BZ induce the phase transition from the rocksalt phase to the monoclinic phase. While for AgBr, the phase transition may be partly attributed to the softening behavior of the TA phonon at the zone boundary X point. Further analysis performed on the elastic constants under pressure suggested that the shear instabilities in C_{44} have no direct relation to the structural phase transition for both compounds.

We thank the China 973 Program for financial support under Grant No. 2005CB724400, the National Doctoral Foundation of China Education Ministry under Grant No. 20050183062, the SRF for ROCS, SEM, and the Program for 2005 New Century Excellent Talents in University. Most of calculations in this work have been done using the PWSCF package.[38]

*Corresponding author. Email address: mym@jlu.edu.cn

[1] E. Hanneman, M. D. Banus, and H. C. Gatos, J. Phys. Chem. Solids **25**, 293 (1964).
[2] S. C. Yu, I. L. Spain, and E. F. Skelton, Solid State Commun. **25**, 49 (1978).
[3] A. Jayaraman, Rev. Mod. Phys. **55**, 65 (1983).
[4] R. J. Nelmes and M. I. Mchmahon, J. Synchrotron Radiat. **1**, 69 (1994).
[5] R. J. Nelmes, M. I. McMahon, and S. A. Belmonte, Phys. Rev. Lett. **79**, 3668 (1997).
[6] Y. E. Tonkov, *High Pressure Phase Transformations. A Handbook* (Gordon and Breach, London, 1992).
[7] S. Hull and D. A. Keen, Phys. Rev. B **59**, 750 (1999).
[8] F. Kirchhoff, J. M. Holender, and M. J. Gillan, Phys. Rev. B **49**, 17420 (1994).
[9] P. W. Bridgman, Proc. Am. Acad. Arts Sci. **74**, 1 (1945).
[10] T. E. Slykhouse and H. G. Drickamer, J. Phys. Chem. Solids **7**, 206 (1958).
[11] R. N. Schock and J. C. Jamieson, J. Phys. Chem. Solids **30**, 1527 (1969).
[12] R. W. G. Wyckoff, *Crystal Structures* (Wiley, New York, 1963).
[13] D. C. Gupta and R. K. Singh, Phys. Rev. B **43**, 11185 (1991).
[14] G. S. Nunes, P. B. Allen, and J. L. Martins, Phys. Rev. B **57**, 5098 (1998).
[15] V. Ozoliņš and Alex Zunger, Phys. Rev. Lett. **82**, 767 (1999).
[16] S. Baroni, S. de Gironcoli, A. Corso, and P. Gianozzi, Rev. Mod. Phys. **73**, 515 (2001).
[17] Y. M. Ma, J. S. Tse, and D. D. Klug, Phys. Rev. B **67**, 140301(R) (2003).
[18] Y. M. Ma, J. S. Tse, and D. D. Klug, Phys. Rev. B **69**, 064102 (2004).
[19] S. Baroni, P. Giannozzi, and A. Testa, Phys. Rev. Lett. **58**, 1861 (1987).
[20] J. P. Perdew and K. Burke, Int. J. Quantum Chem. **57**, 309 (1996).
[21] N. Troullier and J. L. Martins, Phys. Rev. B **43**, 1993 (1991).
[22] Y. Le Page and P. Saxe, Phys. Rev. B **65**, 104104 (2002).
[23] Y. Le Page and J. R. Rodgers, J. Appl. Crystallogr. **38**, 697 (2005).
[24] G. Kresse and J. Hafner, Phys. Rev. B **48**, 13115 (1993); **49**, 14251 (1994); G. Kresse, PhD Thesis (Technische Universität, Wien, 1993).
[25] G. Kresse and D. Joubert, Phys. Rev. B **59**, 1758 (1999); P. E. Blochl, *ibid.* **50**, 17953 (1994).
[26] R. W. G. Wyckoff, *Crystal Structures* (Wiley, New York, 1963).
[27] W. Hidshaw, J. T. Lewis, and C. V. Briscoe, Phys. Rev. **163**, 876 (1967).
[28] P. Lawaetz, Phys. Rev. B **5**, 4039 (1972).
[29] D. S. Tannhouser, L. J. Bruner, and A. W. Lawson, Phys. Rev. **102**, 1281 (1956).
[30] S. N. Vaidya and G. C. Kennedy, J. Phys. Chem. Solids **32**, 951 (1971).
[31] P. R. Vijayaraghavan, R. M. Nicklow, H. G. Smith, and M. K. Wikinson, Phys. Rev. B **1**, 4819 (1970).
[32] B. Dorner, W. von der Osten, and W. Bührer, J. Phys. C **9**, 723 (1976).
[33] W. von der Osten and B. Dorner, Solid State Commun. **16**, 431 (1975).
[34] W. von der Osten, J. Weber, and G. Schaack, Solid State Commun. **15**, 1561 (1974).
[35] W. C. Hughes and L. S. Cain, Phys. Rev. B **53**, 5174 (1996).
[36] K. F. Loje and D. E. Schuele, J. Phys. Chem. Solids **31**, 2051 (1970).
[37] P. T. Jochym and K. Parlinski, Phys. Rev. B **65**, 024106 (2001).
[38] S. Baroni, A. Dal Corso, S. de Gironcoli, and P. Giannozzi, http://www.pwscf.org